chemosensors

MDPI

Supplementary Material

Imidazole-Based Monomer as Functional Unit for the Specific Detection of Paraxanthine in Aqueous Environments

Rozalia-Maria Anastasiadi [1,2], Federico Traldi [2] and Marina Resmini [2,*]

[1] R&D Department of Puratos Hellas, Oinofyta Viotias, 32011, Greece; ranastasiadi@puratos.com
[2] Department of Chemistry, Queen Mary University of London, Mile End Road, London E1 4NS, UK; f.traldi@qmul.ac.uk
* Correspondence: m.resmini@qmul.ac.uk

1. Materials and Methods

1.1. Synthesis of 4-vinylimidazole

The obtained material of 4-vinylimidazole was confirmed by ^{1}H NMR in $CDCl_3$ and the peaks were assigned as follows: δ 7.61 (s, 1H), 7.04 (s, 1H), 6.63 (dd, J=17.6, 11.1 Hz, 1H), 5.67 (d, J=17.6 Hz, 1H), 5.15 (dd, J=11.1, 1.0 Hz, 1H).

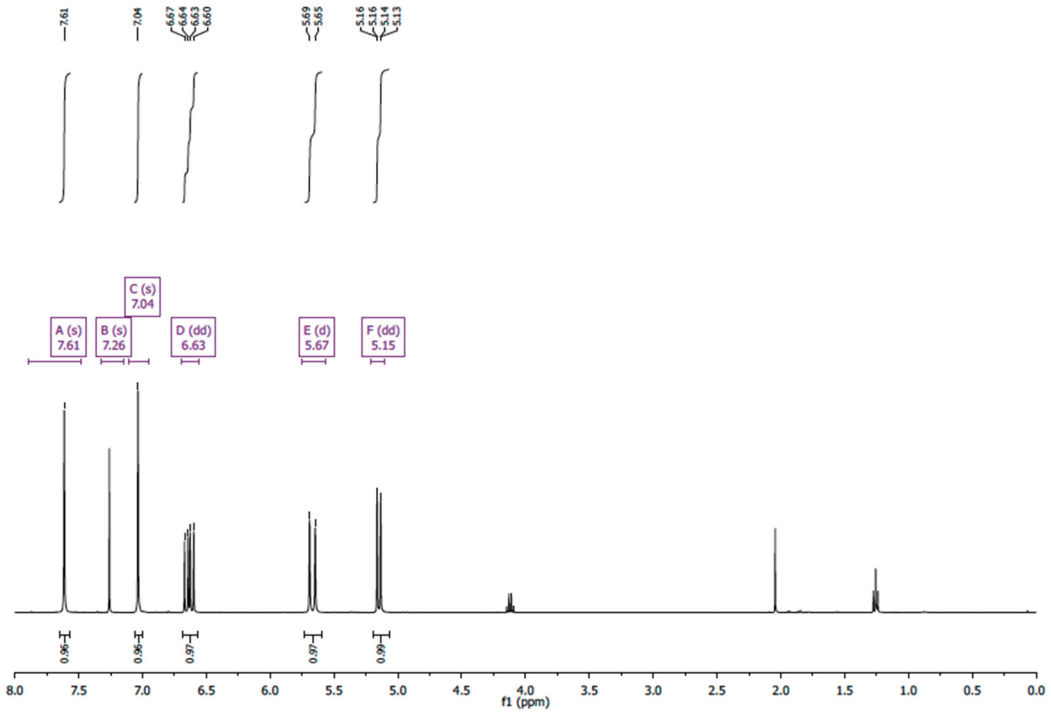

Figure S1. ^{1}H NMR spectrum of 4-vinylimidazole in $CDCl_3$, at 25 °C.

1.2. Synthesis of 4-ethylimidazole

4-Ethylimidazole was obtained by hydrogenation of 4-vinylimidazole and its structure was confirmed by ^{1}H NMR in $CDCl_3$ and the peaks were assigned as follows:

^{1}H NMR (400 MHz, $CDCl_3$) δ 9.33 (s, NH), 7.55 (d, J=1 Hz, 1H), 6.78 (d, J=1 Hz, 1H), 2.65 (qd, J=7.6, 0.8 Hz, 2H), 1.25 (t, J=7.6 Hz, 3H).

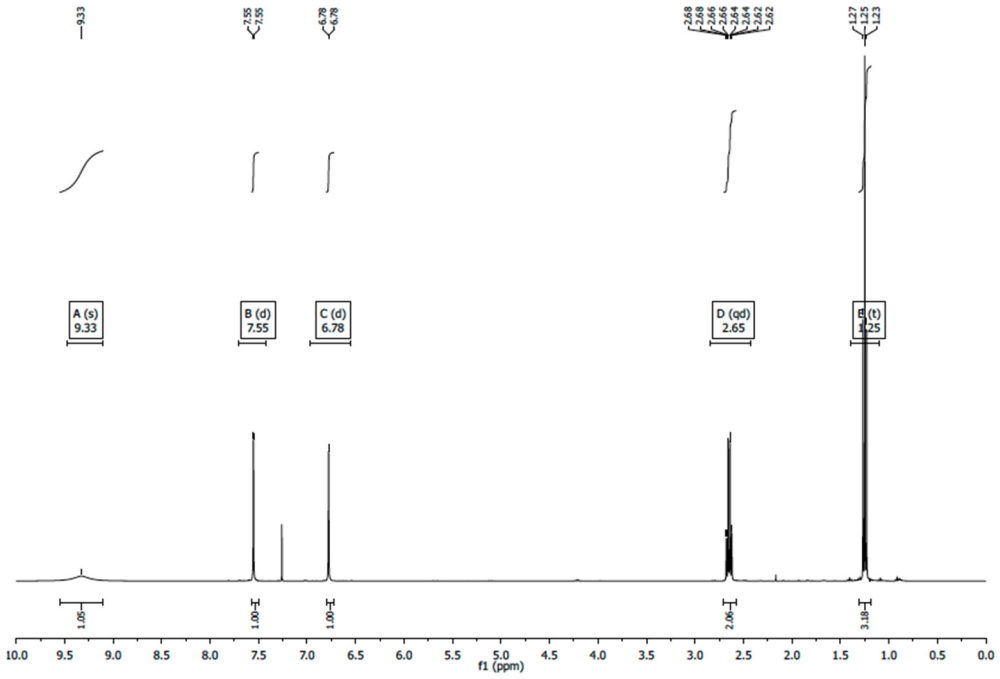

Figure S2. ^{1}H NMR spectrum of 4-ethylimidazole in $CDCl_3$, at 25 °C.

2. Results

Successive amounts of paraxanthine, ranging from 0 to 10 equivalents, or caffeine, ranging from 0 to 5 equivalents were added into a solution of adenine at a concentration equal to 3.7 and 0.4 mM, respectively. The ^{1}H NMR stacked plots are shown in Figure S3 and S4, respectively.

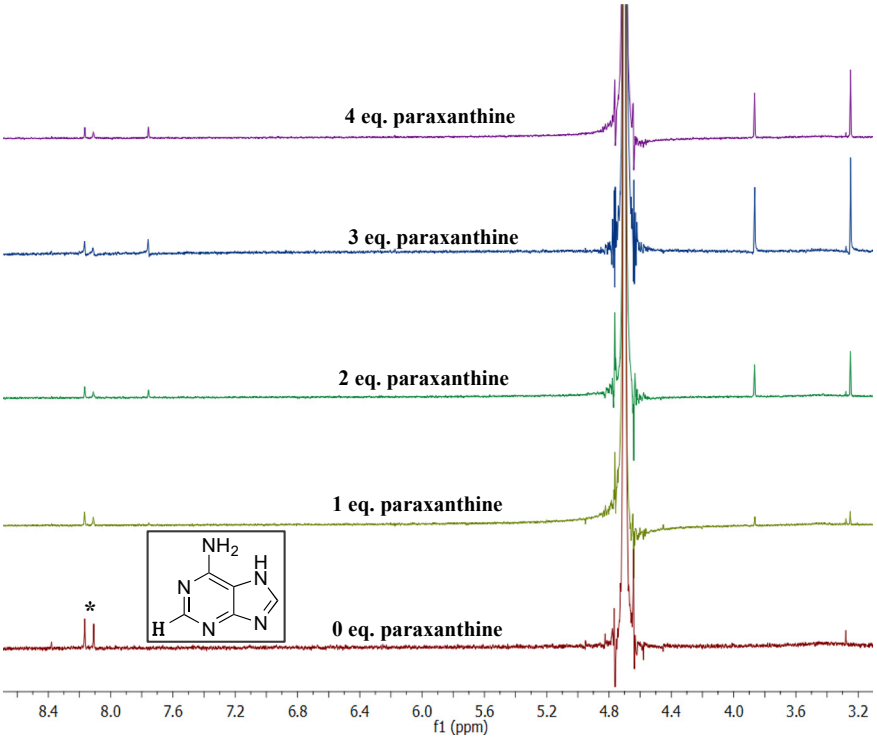

Figure S3. Partial ^{1}H NMR spectra for the titration of adenine (0.4 mM) with increasing amounts of paraxanthine (0–5 equivalents) in D_2O, at 25 °C. The indicated proton of adenine with a star was the one to be monitored.

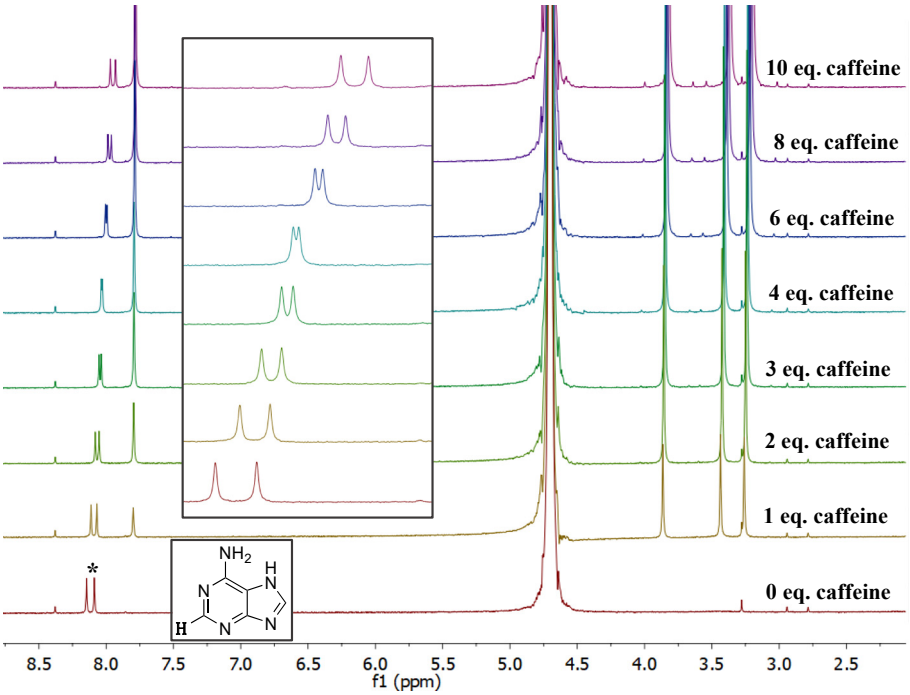

Figure S4. Partial ^{1}H NMR spectra for the titration of adenine (3.7 mM) with increasing amounts of caffeine (0–10 equivalents) in D_2O, at 25 °C. The indicated proton of adenine with a star was the one to be monitored.

The variation of the indicated proton of adenine which showed the largest change in chemical shift for both molecules is shown in Figure S5.

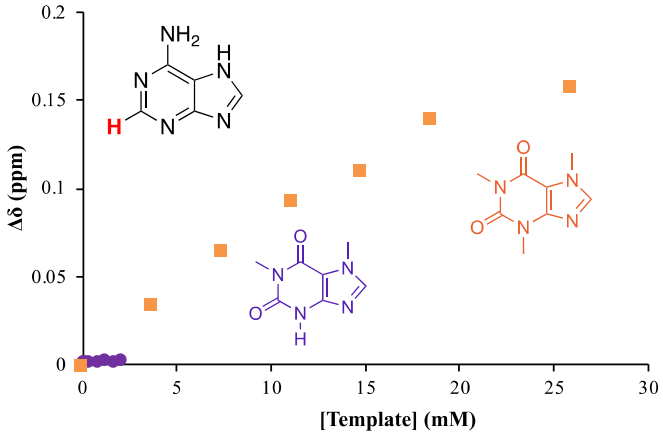

Figure S5. ^{1}H NMR titrations of adenine with paraxanthine (purple circles) and caffeine (orange squares) in D_2O, at 25 °C: variation of the chemical shift of the indicated proton of adenine upon stepwise increase of either paraxanthine (0–5 equivalents) or caffeine concentration (0–9 equivalents). The chemical structures of paraxanthine and caffeine are indicated in purple and orange, respectively.

^{1}H NMR titration was carried out in D_2O by addition of successive amounts of caffeine and paraxanthine from 0 to 9 equivalents into a solution of 5-CQA and the variation of the chemical shift of the indicated proton of 5-CQA is shown in Figure S6.

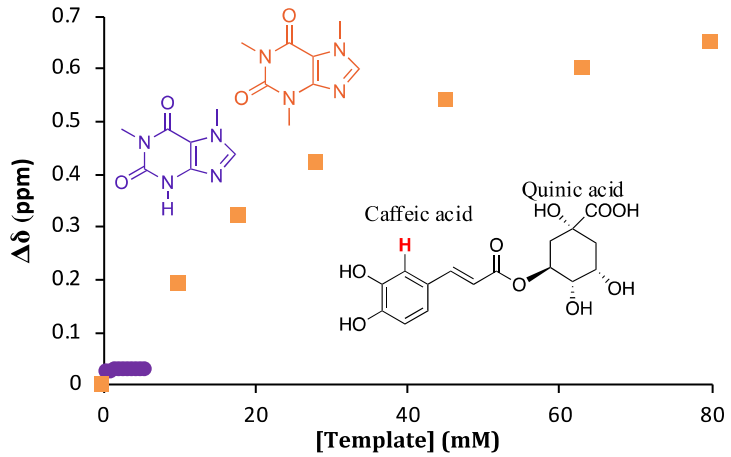

Figure S6. ^{1}H NMR titrations of 5-caffeoylquinic acid (5-CQA) with caffeine in D_2O, at 25 °C: variation of the chemical shift of the indicated proton of 5-CQA acid upon stepwise increase of caffeine concentration (0–9 equivalents). The chemical structure of caffeine is indicated in orange.

In Figure S7 is shown the ^{1}H NMR stacked plot for the variation in chemical shift of the indicated proton of HPTS upon stepwise addition of paraxanthine.

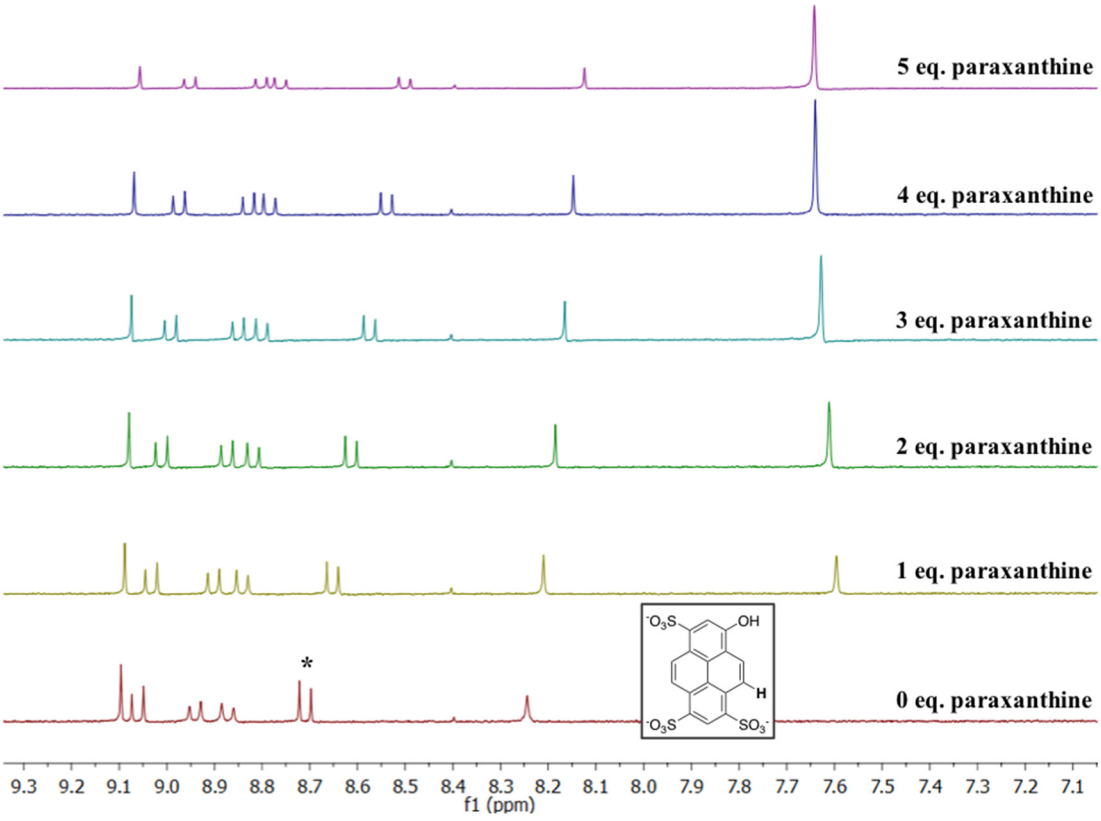

Figure S7. ^{1}H NMR stacked plot (partial ^{1}H NMR spectra) for the titration of HPTS (1.4 mM) with increasing amounts of paraxanthine from 0 to 5 equivalents, in D_2O, at 25 °C. The indicated proton of 8-hydroxypyrene-1,3,6-trisulfonic acid trisodium salt (HPTS) with a star was the one to be monitored.

The variation of the chemical shift for the indicated proton of HPTS upon addition of increasing amounts of either paraxanthine or caffeine is shown in Figure S8.

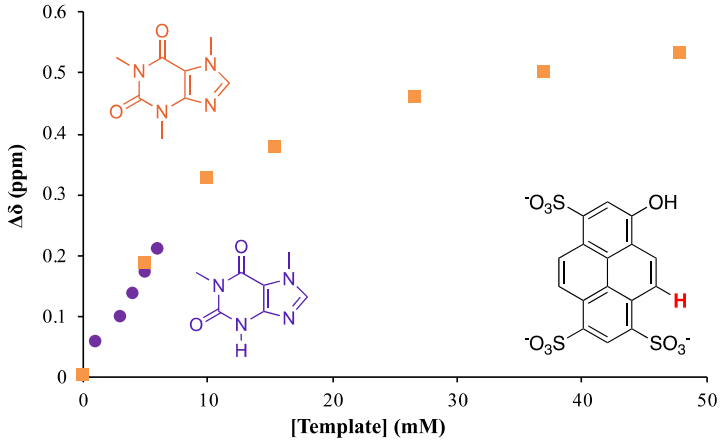

Figure S8. ^{1}H NMR titrations of 8-hydroxypyrene-1,3,6-trisulfonic acid trisodium salt (HPTS) with paraxanthine (purple circles) and caffeine (orange squares) in D_2O, at 25 °C: variation of the chemical shift of the indicated proton of HPTS upon stepwise increase of either paraxanthine (0–5 equivalents) or caffeine concentration (0–9 equivalents). The chemical structures of paraxanthine and caffeine are indicated in purple and orange, respectively.

^{1}H NMR titrations were performed by keeping fixed the concentration of imidazole at 1.5 mM and varying the amount of paraxanthine ranging from 0 to 5 equivalents. The variation of the proton which resulted in the largest chemical shift is shown in the ^{1}H NMR stacked plot in Figure S9.

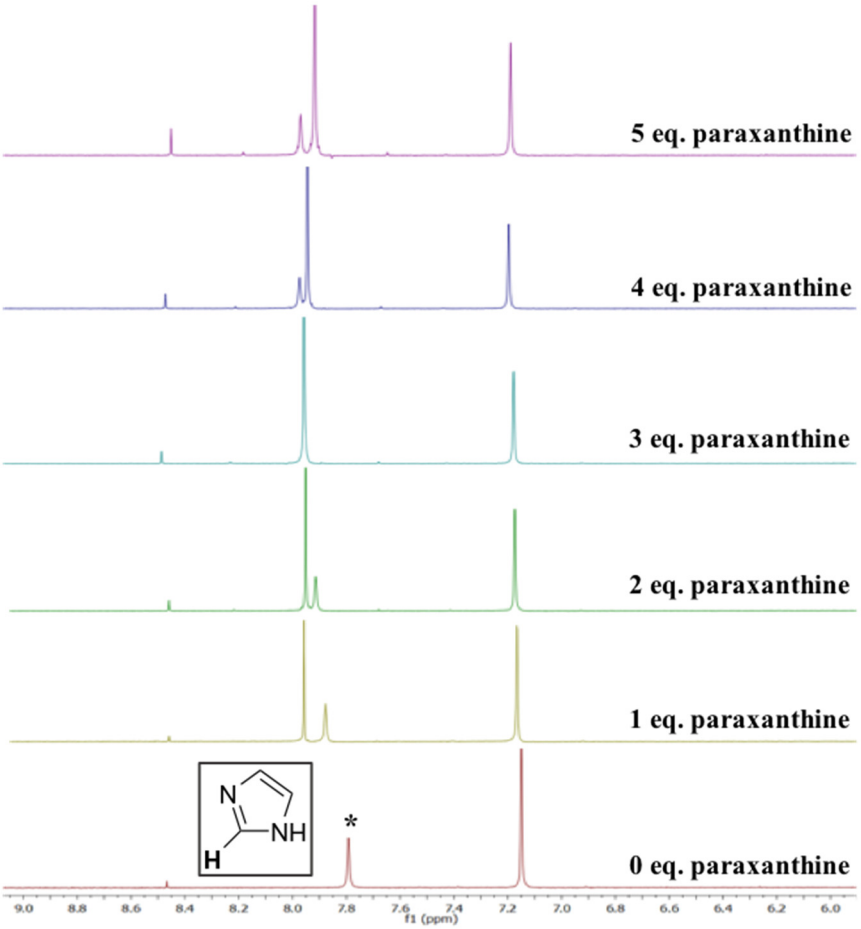

Figure S9. ^{1}H NMR stacked plot (partial 1H NMR spectra) of solutions containing imidazole (1.5 mM) upon stepwise addition of paraxanthine (0–5 equivalents) in D2O, at 25 °C. The indicated proton of imidazole with a star was the one to be monitored.

The raw ITC data of the control heat dilution experiment for imidazole is shown in Figure S10.

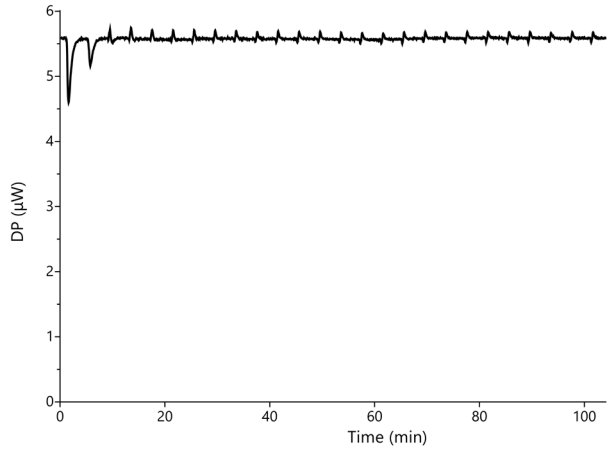

Figure S10. Raw ITC data for the heat dilution (control) experiment of imidazole (20 mM) in water, at 25 °C.

The thermodynamic signature plot of the ITC titration of paraxanthine with imidazole is shown in Figure S11.

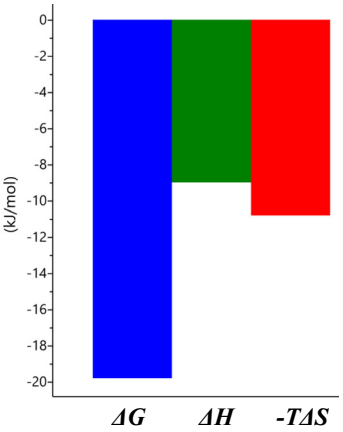

Figure S11. Thermodynamic signature plot (*ΔG, ΔH and -TΔS* values) for the ITC titration of paraxanthine (5.6 mM) upon stepwise injection of imidazole (20 mM) in water, at 25 °C.

The thermodynamic signature plot of the ITC titration of paraxanthine with 4-vinylimidazole is shown in Figure S12.

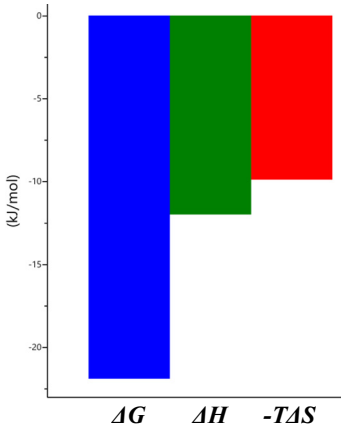

Figure S12. Thermodynamic signature plot (*ΔG, ΔH and -TΔS* values) for the ITC titration of paraxanthine (2 mM) upon stepwise injection of 4-vinylimidazole (10 mM) in water, at 25 ˚C.

The thermodynamic signature plot of the ITC titration of paraxanthine with 4-ethylimidazole is shown in Figure S13.

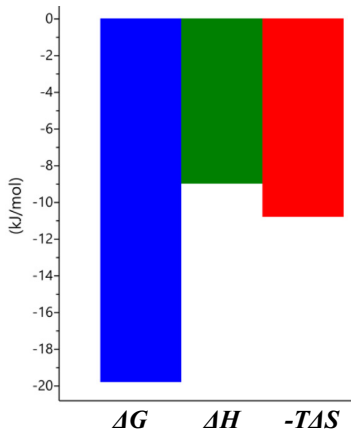

Figure S13. Thermodynamic signature plot (*ΔG, ΔH and -TΔS* values) for the ITC titration of paraxanthine (1 mM) upon stepwise injection of 4-ethylimidazole (20 mM) in water, at 25 ˚C.

The raw data of the ITC titrations of paraxanthine, theophylline, theobromine and caffeine with 4-ethylimidazole are shown in Figure S14.

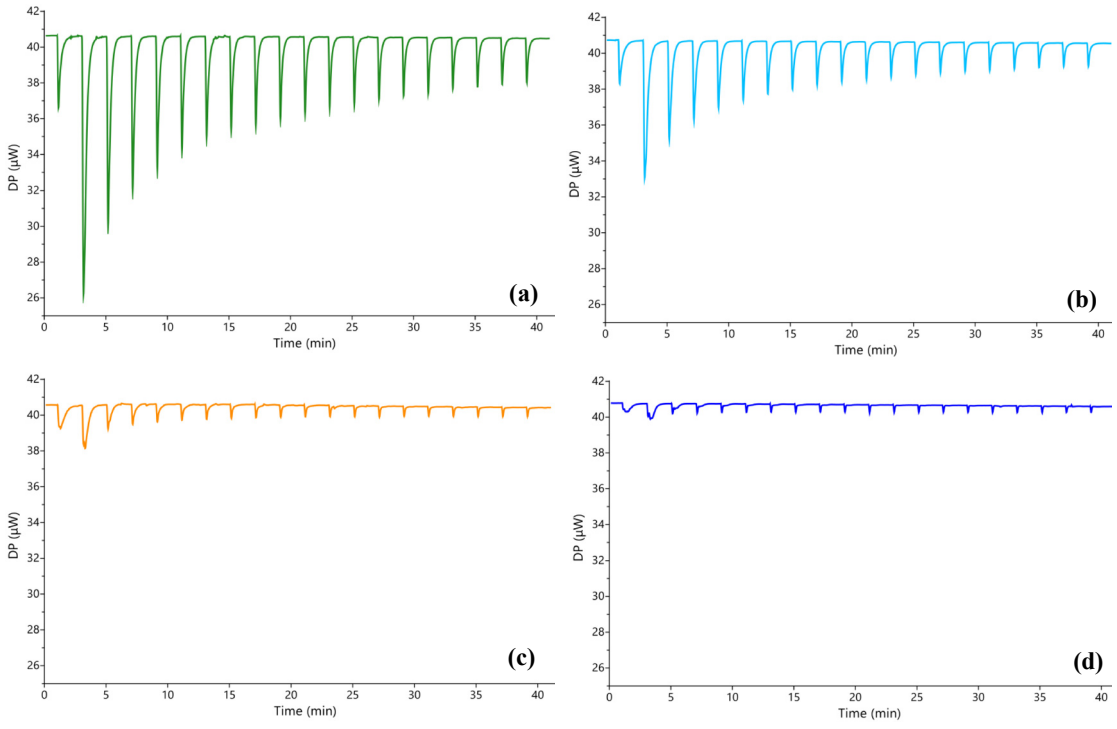

Figure S14. Raw ITC data for the stepwise injection of 4-ethylimidazole (27.8 mM) in: (a) paraxanthine (2.8 mM); (b) theophylline (2.8 mM); (c) theobromine (2.8 mM) and (d) caffeine (2.8 mM) in water, at 25 ˚C.

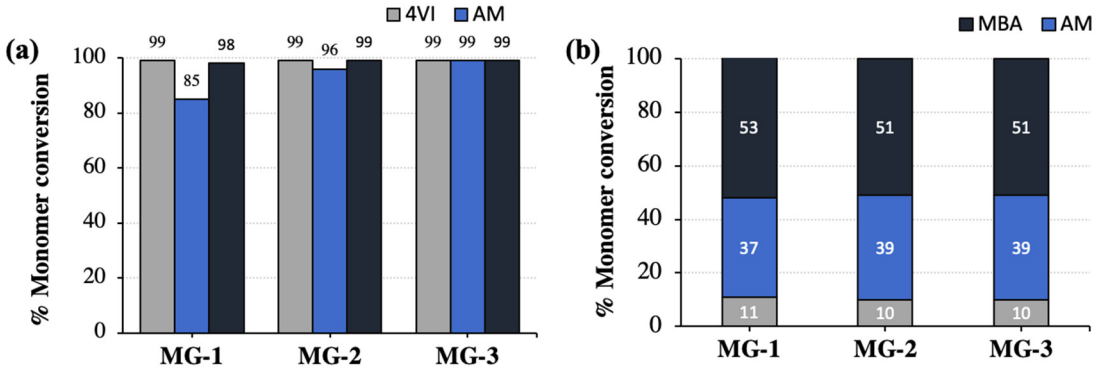

Figure S15. Graphs showing the (a) conversions of 4-vinylimidazole (4VI), acrylamide (AM) and N,N′-methylenebisacrylamide (MBA) determined by ^{1}H NMR and (b) final polymer composition of the obtained microgels. All polymerisations were carried out in D_2O (70 °C, 24 h) at two different C_M values and ammonium persulfate (APS) concentrations.

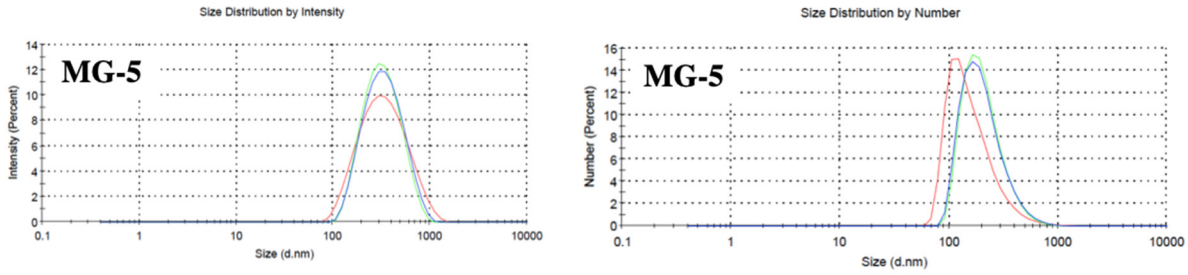

Figure S16. Particle size distribution by intensity and number of MG-5 as measured by dynamic light scattering at a concentration of 0.5 mg/mL in D_2O.

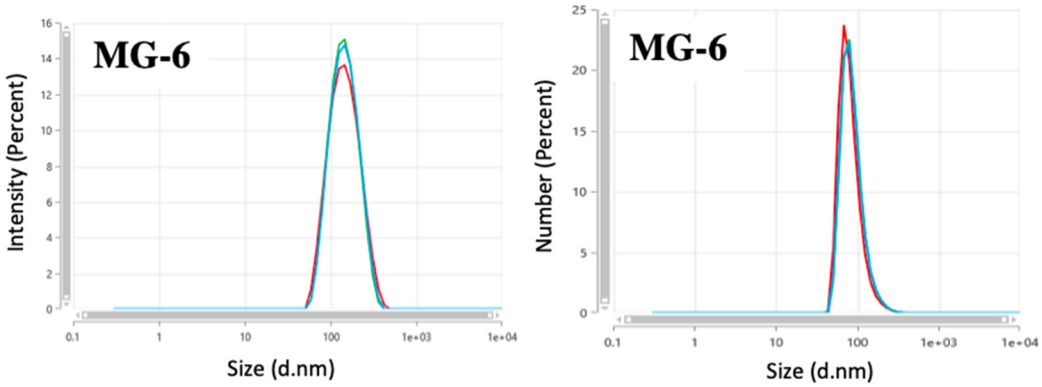

Figure S17. Particle size distribution by intensity and number of MG-6 as measured by dynamic light scattering at a concentration of 0.5 mg/mL in D_2O.

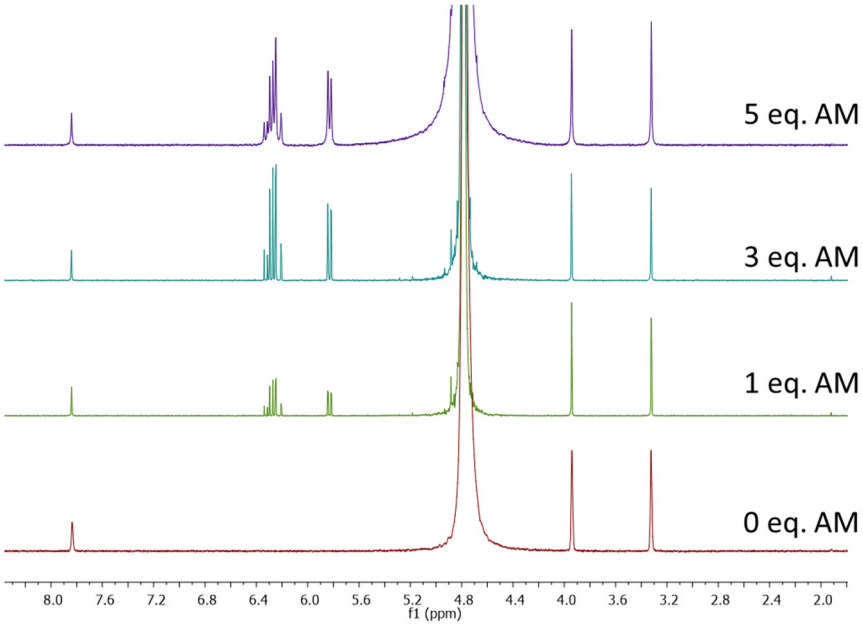

Figure S18. ^{1}H-NMR interaction study between PX (0.5 mg/mL, 2.78 mM) and AM (1-5 equivalents).

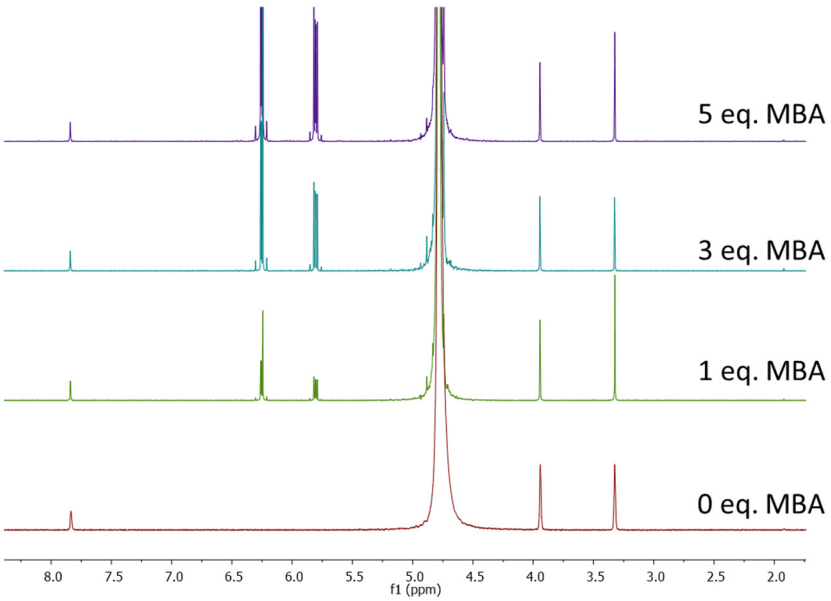

Figure S19. ^{1}H-NMR interaction study between PX (0.5 mg/mL, 2.78 mM) and MBA (1-5 equivalents).

The interaction between backbone monomer AM and the crosslinker MBA with PX was studied with ^{1}H-NMR. PX was dissolved in D_2O at a concentration of 0.5 mg/mL (2.78 mM). Then, different aliquots of either AM or MBA solutions in D_2O were added to obtain final monomer concentrations of 1, 3 or 5 equivalents. ^{1}H-NMR spectra were then recorded and chemical shifts (δ) of the protons of PX monitored. All spectra were obtained at 25°C.